

2018-10

# Application of field-portable-XRF for the determination of trace elements in deciduous leaves from a mine-impacted region

Turner, Andrew

<http://hdl.handle.net/10026.1/12203>

---

10.1016/j.chemosphere.2018.06.110

Chemosphere

Elsevier

---

*All content in PEARL is protected by copyright law. Author manuscripts are made available in accordance with publisher policies. Please cite only the published version using the details provided on the item record or document. In the absence of an open licence (e.g. Creative Commons), permissions for further reuse of content should be sought from the publisher or author.*

1  
2  
3 **Application of field-portable-XRF for the determination**  
4 **of trace elements in deciduous leaves from a mine-**  
5 **impacted region**  
6  
7

8 **Andrew Turner<sup>\*1</sup>, Chor Chi Chan<sup>1</sup>, Murray T. Brown<sup>2</sup>**

9  
10 *<sup>1</sup>School of Geography, Earth and Environmental Sciences and <sup>2</sup>School of Biological and*  
11 *Marine Sciences, Plymouth University, Drake Circus, Plymouth PL4 8AA, UK*  
12  
13  
14

15 <sup>\*</sup>Corresponding author: e-mail: aturner@plymouth.ac.uk  
16  
17

18 Accepted in Chemosphere 21 June 2018

19 <https://doi.org/10.1016/j.chemosphere.2018.06.110>

20 Embargoed until 21 June 2019  
21

## Abstract

Deciduous leaves ( $n = 87$ ) from beech (*Fagus sylvatica*), birch (*Betula* spp.) and oak (*Quercus* spp.) trees have been collected from three metal mine-impacted sites in southwest England and tested for concentrations of trace elements (As, Cu, Pb and Zn) using a field-portable-x-ray fluorescence (FP-XRF) spectrometer configured in a low density mode and housed in a stand. When intact leaves were analysed directly, mean detection limits ranged from about 10 (As) to 70  $\mu\text{g g}^{-1}$  (Cu) on a fresh weight basis; after freeze-drying, respective limits increased to about 20 and 120  $\mu\text{g g}^{-1}$  on a dry weight basis. Within these constraints, As and Zn were detected in samples from all genera, with concentration differences between fresh and dry states attributed to the mass of water present and its propensity to attenuate x-rays. A comparison with As and Zn concentrations in local soils and determined by XRF in a higher density mode revealed different accumulation and exclusion characteristics among the three genera of tree. In contrast, and despite soil concentrations that were similar to those of Zn, Cu was detected in only two dried leaves and Pb evaded detection throughout. Pooled results from the study showed good agreement with independent results derived from ICP following acid digestion, with a slope that was close to unit value. Accordingly, the XRF approach is able to provide a rapid assessment of the levels of certain trace elements in leaves from contaminated sites, with the configuration deployed on site having potential to deliver immediate results.

**Keywords:** deciduous leaves; field-portable-XRF; arsenic; zinc; soils; biomonitoring

## 1. Introduction

Although mosses and epiphytic lichens have gained widespread use in biomonitoring of airborne trace element pollution, their absence in some urban and industrialised areas has resulted in the study of higher plants (Bargagli et al., 2003; Aničić et al., 2011; Serbula et al., 2014). Many tree species are tolerant of high environmental concentrations of trace elements and leaves are often the main sink for pollutants (Bargagli, 1998). Thus, as well as providing a means of increasing the trace element content of top soils through leaf deposition-decomposition and increasing trace element exposure to consuming organisms, leaves act as potential indicators of both contaminated soil, through uptake via the root system, and polluted air, through wet and dry deposition (Franiel and Babczyńska, 2011; Dimitrijević et al., 2016; Pająk et al., 2017).

At sites impacted by contemporary or historical metalliferous mining, and where the presence of elevated environmental concentrations of many trace elements is a concern, deciduous and evergreen tree leaves have been commonly employed as indicators of soil contamination (Unterbrunner et al., 2007; Dmuchowski et al., 2014; Nirola et al., 2015; Stefanowicz et al., 2016). Here, capture and uptake of a trace element is from a large soil volume, with the concentration of an element in the leaves reflecting the availability of the element in the soil rather than its total concentration. Strictly, and to act as a true bioindicator, uptake through the roots should be relatively constant over a wide gradient of trace element concentrations in the soil such that there should be a linear relationship between concentrations in the leaves and in the soil (Baker et al., 2000; Kabata-Pendias and Pendias, 2001). However, some trees may act as excluders for certain elements by inhibiting their uptake into roots, even at high external concentrations in the soil, while others may act as hyper-accumulators which are able to tolerate high concentrations in their leaves, even at low external concentrations (Madejón et al., 2004; Schmidt et al., 2016); the latter are,

therefore, particularly attractive as phytoremediators of highly contaminated soils (Antosiewicz et al., 2008; Dimitrijević et al., 2016).

With different possible sources of trace elements (from the atmosphere and soil) and potentially confounding issues of hyper-accumulation and exclusion, the analysis of a large number of leaf samples is often required at contaminated sites, with repeat visits sometimes necessary. Conventional analysis of leaves involves digestion of the matrix in concentrated mineral acid followed by trace element determination by, for example, inductively coupled plasma spectrometry or atomic absorption spectrometry, but this approach can be time- and resource-consuming and generate large quantities of hazardous waste. As an alternative, plant material may be determined non-destructively by x-ray fluorescence (XRF) spectrometry. Here, samples are typically dried, milled and packed before being excited by an x-ray beam, with the expulsion of inner electrons of an atom accompanied by electrons cascading from higher orbitals and the emission of characteristic fluorescent x-rays (Sacristán et al., 2016; Towett et al., 2016).

In order to further minimise sample preparation, it may be assumed that the plant matrix has similar characteristics to thin plastic films in terms of the absorption, scattering and fluorescence of x-rays, and analyse material intact (i.e. without milling or packing) using an XRF algorithm that is calibrated for low density matter. This approach was recently tested and validated both in the laboratory and in the field on coastal and marine macroalgae (Bull et al., 2017; Turner et al., 2017) and is trialled in the present study on deciduous leaves. Specifically, the current investigation focuses on the trace metalloid, As, and the trace metals Cu, Pb and Zn, in both common leaves and in soils (with the latter employing more established XRF protocols) at three sites impacted by historical, non-ferrous mine waste.

Although tests were performed solely in the laboratory, the potential for applying the approach in the field is also addressed.

## **2. Materials and methods**

### *2.1. Sampling*

Sampling of leaves and soils was undertaken at three sites impacted by historical (19<sup>th</sup> century), non-ferrous metal mining activities in west Devon, south west England. The geology of the region is dominated by fine-grained sedimentary sequences and chert but with outcrops of granite and slates, and soils are mainly brown earths that are well-drained but subject to slight seasonal waterlogging (Rawlins et al., 2003). The region is sparsely populated, with occasional small settlements and farms, and current land use is dominated by agriculture and managed woodland. The first site (S1) was on Dartmoor National Park in the vicinity of a series of relatively small, disused copper mines (digital co-ordinates: 50.5130, -4.1116; 85 m asl). The second and third sites were within the UNESCO district of the Tamar Valley at locations influenced by more extensive mining and processing facilities for both copper and arsenic; specifically, S2 was adjacent to an old but functional adit (50.5361, -4.2081; 50 m asl) and S3 was along the northern edge of a large spoil tip (50.5385, -4.2214; 78 m asl).

Each site was visited during mid-autumn (early November) in 2016, following a period of dry weather and as deciduous foliage was being shed. A total of 87 leaves were collected by hand and using plastic tweezers from trees that were common to all sites and that usually occurred in clusters but were occasionally solitary: namely, beech (*Fagus sylvatica*), birch (*Betula* spp., including *B. pendula*) and oak (*Quercus* spp.). Specifically, three leaves were taken from lateral branches at a height of about 2 m from between one and five trees of each genus (depending on their abundance and accessibility) and stored in individual zip-lock

specimen bags in a dark polyethylene box. Soil samples, of about 300 g and to depths of around 10 cm, were collected from under the canopies of three trees from each location using a plastic trowel and were stored likewise.

## *2.2. Leaf sample processing and XRF analysis*

On return to the laboratory, leaf surfaces were wiped gently with three-ply blue roll to remove any visibly adherent material and weighed on a five-figure Sartorius balance. Fresh samples were then analysed for a suite of elements, of which As, Cu, Pb and Zn as important contaminants of non-ferrous mining are the focus of the present study, by energy dispersive, field-portable (FP-)XRF using a battery-powered Niton XRF analyser (model XL3t 950 He GOLDD+) which was configured, nose-upwards, in a bench-top accessory stand and activated remotely by a laptop connected via USB. In order to minimise any artefacts arising from variations in geometry or thickness, an area of the upper blade midway between the mid-rib and margin, and free from any sign of infection, was selected for analysis. This area was measured for thickness using Allendale digital callipers before being positioned directly above the XRF detection window, a process aided by imagery from an integrated CCD camera and, where necessary, polyethylene blocks outside of the x-ray beam acting as weights. Once the shield of the stand was closed, measurements, with appropriate thickness correction and in a low-density plastics mode, were undertaken for equal counting periods in a main energy range (50 kV/40  $\mu$ A) and low energy range (20 kV/100  $\mu$ A). Counting was trialled up to ten minutes but a total period of 120 seconds was selected as a suitable timescale that appeared to provide sufficiently low counting errors yet maximise the number of elements detected. Spectra arising from both energy ranges were quantified by fundamental parameters to yield elemental concentrations in  $\mu\text{g g}^{-1}$  and a counting error of  $2\sigma$  (95% confidence) that were downloaded to the laptop using Niton Data Transfer software.

In order to correct for the mass contribution of water and to evaluate the effects of the aqueous phase on x-ray absorption, leaves were frozen, dried for 24 h in an Edwards Super Modulyo freeze-drier and reweighed before being re-analysed at the approximate positions measured while fresh. With no suitable biological reference films available, performance and precision were evaluated by analysing a Niton plastic reference disc (PN 180-619, LOT#T-18) certified for a suite of elements (including As and Pb) at regular intervals during each measurement session.

### *2.3. Soil sample processing, characterisation and XRF analysis*

Soil samples were freeze-dried for 48 h before being ground with a ceramic pestle and mortar and sieved through a 63  $\mu\text{m}$  stainless steel sieve. A sufficient quantity of each fractionated sample was then used to completely fill a series of Chemplex series 1400 XRF sample cups (21-mm internal diameter) that were collar-sealed with 3.6  $\mu\text{m}$  SpectraCertified Mylar polyester film. For XRF analysis, cups were placed centrally over the detector window with the collar-sealed Mylar surface face-down, and measurements were conducted for 60 seconds in a higher density mining mode, comprising successive counting periods of 20 s each in a main (50 kV/40  $\mu\text{A}$ ), low (20 kV/100  $\mu\text{A}$ ) and high (50 kV/40  $\mu\text{A}$ ) energy range. Spectra were quantified and concentrations downloaded to the laptop as above. For quality assurance purposes, sufficient quantities of a Sigma-Aldrich RTC loam certified for As and Zn (MSL-MSL101) and a National Institute of Standards and Technology soil certified for a broader suite of elements (SRM 2709a) were packed into XRF cups and analysed likewise.



Ten g portions of the remaining fractionated soil samples were equilibrated with 25 ml aliquots of deionised water in a series of 50 ml polypropylene centrifuge tubes and the pH measured using a Meterlab PHM210 pH meter and Hach pH2051-8 electrode.

#### *2.4. Leaf digestion and analysis by ICP*

As an independent and more sensitive measure of the metal and metalloid content of leaves, dried and infection-free whole leaf samples ( $n = 28$ ) from different trees and sites and, in triplicate, a powdered leaf reference material (GBW 08501, peach leaves) were acid-digested and analysed by inductively coupled plasma-mass spectrometry (ICP-MS). Thus, samples were accurately weighed into individual Teflon tubes to which 6 ml aliquots of  $\text{HNO}_3$  (Fisher Chemical TraceMetal<sup>TM</sup> Grade) were added. The contents were digested in a CCEM MARS 5 XPRESS microwave at 1600 W for 45 min before being allowed to cool. Digests were then washed into individual 25 ml volumetric flasks and diluted to mark with Millipore Milli-Q water.

Digests were analysed for As, Cu, Pb and Zn using a collision cell-ICP-MS (Thermo X-series II, ThermoFinnigan, Winsford, UK) with a concentric glass nebuliser and conical spray chamber. RF power was set at 1400 W and coolant, auxiliary, nebuliser and collision cell gas flows rates were 13 L Ar min<sup>-1</sup>, 0.70 L Ar min<sup>-1</sup>, 0.786 L Ar min<sup>-1</sup> and 3.5 mL 7%  $\text{H}_2$  in He min<sup>-1</sup>, respectively. The instrument was calibrated externally using four standards prepared by dilutions of a QC 26 multi-element solution (CPI International, Amsterdam) in 0.1 M  $\text{HNO}_3$ , and internally by the addition of 100  $\mu\text{g L}^{-1}$  of In and Ir to all samples and standards. Data were acquired over a dwell period of 10 ms, with 50 sweeps per reading and three replicates and were converted to dry weight concentrations (in  $\mu\text{g g}^{-1}$  dw) from the volume of diluted digest and mass of leaf digested. Limits of detection on this basis were < 0.5  $\mu\text{g g}^{-1}$  for all elements analysed.

## 2.5. Quality assurance

Dry weight concentrations arising from XRF or ICP analyses of the various reference materials (plastic disc, soils and leaves) are compared with certified or indicative values in Table 1. Thus, within the levels of uncertainty and error, agreement was accomplished by XRF for As and Pb in polyethylene and As and Zn in NIST soil and by ICP for As, Pb and Zn in peach leaves, with mean measured concentrations in the remaining cases within 25% of the respective mean certified values. Precision, as one standard deviation relative to the mean, was < 5% in all cases with the exception of Zn in peach leaves (15%) and As, Cu and Pb in NIST soil (between 13 and 24%).

## 3. Results and Discussion

### 3.1. Leaf and soil characteristics

Table 2 shows the number of leaves taken from each genus of tree at each site, where multiples of three reflect the number of trees sampled. Overall, 87 samples were collected for analysis with a roughly equal distribution among genera but differences between sites that reflected tree abundance and accessibility. At S1, average leaf size, based on fresh weight, decreased in the following order: *Quercus* > *Fagus* > *Betula*; at S2 and S3, tree growth appeared to be more stunted and the size of oak and beech leaves were reduced considerably such that average leaf size across the three genera was similar. The percentage contribution of water to leaf mass averaged 42% for *Fagus* and *Betula* and 21% for *Quercus*, with leaves in the latter genus being distinctly drier at S2 and S3. Leaf thickness through the measurement area was not significantly different ( $p > 0.05$  according to a series of paired or two-sample  $t$ -tests performed in Minitab v17) between genus, sampling site, or fresh and dry

state, with overall averages of 0.26 mm, 0.27 mm and 0.34 mm for *Betula*, *Fagus* and *Quercus*, respectively.

The pH of the soil samples, together with trace element content determined by XRF in a conventional and established soils mode (Kalnicky and Singhvi, 2001; Radu and Diamond, 2009), are summarised in Table 3. Thus, average pH ranged from about 4.9 to 5.5, with individual measurements ranging from about 3.9 at S2 to 6.3 at S1. Average concentrations of Pb and Zn were similar among the three sites, with individual concentrations ranging from about 70 to 300  $\mu\text{g g}^{-1}$  dw and 90 to 290  $\mu\text{g g}^{-1}$  dw, respectively. In contrast, and consistent with the relative significance of historical mining for Cu and As and legacy contamination, mean concentrations of Cu were three- to four-fold higher and mean concentrations of As about 50 and 130 times higher at S2 and S3 than corresponding mean concentrations at S1.

### 3.2. XRF detection limits in leaves

For a specific counting time and mode of application, the Niton FP-XRF provides measurement limits of detection (LODs) for each element that are dependent on the characteristics of the sample, including its density, thickness and chemical composition, and that are calculated from three counting errors arising from the analysis (or  $2\sigma \times 1.5$ ; 99.7% confidence interval). LODs for As, Cu, Pb and Zn for all samples analysed in the present study are summarised in Table 4, with concentrations given on a fresh weight (fw) or dry weight (dw) basis depending on the nature of sample processing. Thus, for a given element, LODs span about an order of magnitude, with values generally related to the reciprocal of sample thickness, but that were not significantly different ( $p > 0.05$  according to one-way ANOVA performed in Minitab v17) between the different genera of tree. For all elements, average LODs were at least 50% greater for leaves analysed freeze-dried than when fresh. With thicknesses that were statistically indistinguishable between the dry and

fresh states and the propensity of water to absorb low energy x-rays, this observation is, perhaps, counterintuitive. However, based on similar observations made during the XRF analysis of fresh and dried macroalgae (Turner et al., 2017), we attribute the discrepancy to a greater flexibility of biological material when fresh, allowing blades to be positioned closer to the detector window of the instrument. This effect also resulted in precisions, derived from repeat measurements of the same leaf area, that were better when samples were analysed in the fresh state (between 10 and 20%) than when analysed after freeze-drying (between 15 and 25%).

### *3.3. Elemental concentrations in leaves*

Table 5 gives the number of cases that As, Cu, Pb and Zn were detected in the leaf samples along with summary statistics for the resulting concentrations. Using FP-XRF, As was detected in 13 samples when analysed dry with concentrations ranging from about 13 to 360  $\mu\text{g g}^{-1}$  dw, and detection was limited to samples taken adjacent to the spoil heap (S3) and was dominated by oak leaves ( $n = 8$ ). The metalloid was detected in 19 samples when analysed fresh, with concentrations ranging from about 5 to 450  $\mu\text{g g}^{-1}$  fw and, after correction for the amount of water present, from about 12 to 500  $\mu\text{g g}^{-1}$  dw. Detection exhibited a similar site and genus distribution to the dried samples but a number of positives were returned for samples of birch taken at S1.

Zinc was detected in 47 samples analysed dry with concentrations ranging from about 30 to 660  $\mu\text{g g}^{-1}$  dw, and both detection and the highest concentrations were most frequent among birch leaves from S1 and S3. When analysed fresh, Zn was detected in 40 samples and at concentrations ranging from about 20 to 280  $\mu\text{g g}^{-1}$  fw and, after correction for water content, from about 30 to 440  $\mu\text{g g}^{-1}$  dw, with a similar site and genus distribution to that derived from analysis of the dried samples. Copper was detected by XRF in just two dried

oak leaves from S3, despite lower measurement detection limits for the metal in fresh leaves (Table 4), and Pb was never detected by the instrument.

Also shown in Table 5 are concentrations of As, Cu, Pb and Zn returned by ICP following acid digestion of a selection of whole, freeze-dried leaves ( $n = 28$ ) that encompassed each genera from all three sites. Here, each element was detected in all samples tested, with results spanning greater concentration ranges than the corresponding results returned by XRF.

### *3.4. Comparison of concentrations derived from fresh and dry analyses of leaves*

In order to evaluate the impacts of internal water on the results, hence the feasibility of measuring elements in fresh leaves by XRF on site, concentrations returned directly for freeze-dried leaves are compared with dry weight concentrations derived indirectly from the analysis of fresh samples and after correction for water content in Figure 1 (note that the comparison is restricted to cases where detection was accomplished by both approaches on the same sample;  $n = 11$  for As and  $n = 32$  for Zn). Thus, despite different geometries and distances from the detector window incurred by the two states, potential differences in the precise location of sample analysed on successive occasions and the heterogeneous distribution of water within leaves, both data sets exhibited a high degree of association when subject to Pearson's moment correlation analysis performed using the data analysis ToolPak in Excel 2016 ( $r > 0.85$ ,  $p < 0.001$ ). Linear regression analysis performed in Excel 2016 also revealed equations of best fit with either a y-intercept or that were forced through the origin that were highly significant ( $p < 0.001$ ), but regression slopes indicated concentrations that were not equivalent. Specifically, the gradient defining the fresh to dry converted concentrations versus dry concentrations determined directly were either above (As) or below (Zn) unit value.

In addition to its contribution to leaf mass and its alteration of sample geometry, water may influence dry weight concentrations derived from fresh analyses through the absorption of primary and secondary x-rays, an effect whose potential significance can be evaluated theoretically. Thus, the mass attenuation coefficient for water at 10 keV, or the approximate energies of the main K-level emission lines for both As and Zn, is  $5.3 \text{ cm}^2 \text{ g}^{-1}$  (Hubbell and Seltzer, 1996). This yields a half-value layer (where 50% of incident radiation is attenuated) of about 1.3 mm, and attenuation of 10% for a layer of about 0.4 mm, or the upper thickness of the leaves tested. Most leaves that were Zn-positive when analysed both fresh and dry (and as plotted in Figure 1) were from *Betula* spp., whose internal water content was about 60%, while those that were As-positive when analysed in both states were from *Quercus* spp., whose water content was about 20%. On this basis, therefore, we would predict the analysis of fresh samples of consistent thickness to affect the results for Zn to a greater extent than those of As, largely through the absorption of both irradiating and fluorescent x-rays by samples of a higher water content. This assertion is qualitatively consistent with the data in Figure 1 in that the regression slopes for Zn are smaller than those for As, but does not explain why the slope for As lies above unit value. A confounding issue in this respect is the presentation of a flatter and more uniform surface that is closer to the detector when samples are fresh and more pliable, and as described above.

### 3.5. Comparison of concentrations derived by XRF and ICP analyses of leaves

A comparison of the results obtained by ICP, following digestion in concentrated  $\text{HNO}_3$ , with those returned by the FP-XRF revealed no false negatives or false positives; that is, lack of detection by the XRF was not accompanied by a measurement by ICP that exceeded the corresponding LOD of the Niton XL3t and concentrations returned by the XRF were never accompanied by ICP measurements that were below detection limit of the mass

spectrometer. Where concentrations were returned by both ICP and XRF (either on fresh leaves or freeze-dried samples), results are plotted in Figure 2, with As and Zn data shown individually and, with Cu, in combination. Despite the potential limitations and sources of error of XRF outlined above and fundamental discrepancies in the leaf part examined (XRF probes a small area of blade while ICP necessitates digestion of the whole sample), both correlation and linear regression analyses performed in Excel 2016 revealed a significant relationship between the results from both analytical approaches in all cases ( $p < 0.001$ ). Agreement between XRF and ICP, defined as the deviation of the gradient of the regression equation (forced through the origin) from unit slope, was within 30% for both As and Zn and within 10% when data for all trace elements were pooled. In all cases, however, closer agreement resulted when leaves were analysed fresh than when dry, an effect that may be related to the ability to manoeuvre samples closer to the detector window when in the fresh state than after freeze-drying (see above).

### *3.6. Potential application of FP-XRF for biomonitoring*

The present study has explored the feasibility of measuring trace elements in common deciduous leaves directly and non-destructively by FP-XRF. The approach is capable of determining many key elements to dry weight concentrations of a few tens of  $\mu\text{g g}^{-1}$  and is particularly suited to environments where there are clear and significant sources of contaminants. Of the metals and metalloids considered herein, As, a toxic metalloid, and Zn, a micronutrient, were most readily detected in a variety of leaf samples from three sites, and agreement with concentrations derived independently from ICP following acid digestion was sufficiently strong and significant to at least partly satisfy the EPA definitive level data criterion (Environmental Protection Agency, 2007). Being capable of measuring elements in fresh samples, with conversion of concentrations to a dry weight basis accomplished to a good approximation by correction for internal water content, the method has the potential for

monitoring in the field. Here, the instrument would be configured in a portable test stand as described elsewhere (Turner et al., 2017) and activated remotely using a laptop under the operating conditions outlined above. With the simultaneous capability of measuring trace metals and metalloids in soils, the approach can deliver a rapid assessment of site contamination, element compartmentalisation and uptake-exclusion-accumulation.

Although the principal objectives of the study were to explore the potential application of FP-XRF to the biomonitoring of leaves, the results have demonstrated differences in element accumulation among the three genera of tree that were most significant at S3 and as illustrated by the direct measurements of dried samples in Figure 3. Thus, here, As was highly enriched in local soils (Table 3) because of the historical mining for the metalloid but concentrations were two or three orders of magnitude lower in the leaves analysed; specifically, As was detected in two samples of *Fagus* and *Betula* spp. but was detected in all samples of *Quercus* spp. It would appear, therefore, that at least the first two genera are excluders of As in that, despite extremely high concentrations in local soils, there is active inhibition by the root system. In contrast, Zn at S3 exhibited no elevated contamination in soil relative to concentrations at S2 and S3 (Table 3) and, unlike As, showed no measurable accumulation by *Quercus* spp. leaves. However, the metal was detected in every sample of *Betula* and at concentrations that always exceeded the mean concentration of Zn in local soil and that are considered to exert toxic effects on many species (Barker and Pilbeam, 2010). This observation is consistent with the recent assertion that *Betula* spp., and in particular, *B. pendula*, should be classified as hyperaccumulators of Zn, thereby having potential for Zn phytoremediation (Dmuchowski et al., 2014). Presumably, Pb evaded detection throughout the study because translocation from the roots is limited for many tree species, while restricted detection of Cu may be attributable to absorption that is often competitively inhibited by Zn (Kabata-Pendias and Pendias, 2001).



377

378 The observations for As and Zn described above are likely the result of differences in the  
379 accumulation, regulation, tolerance, translocation, exclusion and contribution of atmospheric  
380 deposition between the two elements and among the tree genera. Although determination of  
381 the precise causes for the contrasting behaviours of As and Zn would require further  
382 investigation, this study has clearly demonstrated the usefulness of FP-XRF in rapidly  
383 identifying such issues and its potential for guiding research iteratively and strategically.

384

### 385 **Conclusions**

386 This study has shown that FP-XRF configured in a low density mode is capable of  
387 determining certain trace elements, and in particular, As and Zn, on intact leaves from  
388 contaminated sites. With detection limits of a few tens of  $\mu\text{g g}^{-1}$  in both the fresh and dry  
389 states and good agreement with independent results from ICP analysis, the approach is  
390 suitable for the rapid throughput of samples with minimal preparation. As such, and when  
391 combined with a portable test stand, it also has the potential to be applied on site as a  
392 biomonitoring tool or for directly guiding a research plan strategically.

393

### 394 **Acknowledgements**

395 We are grateful to Drs Andrew Fisher and Alex Taylor, PU, for technical support throughout  
396 the study. This study was funded partly by a HEIF V Marine Institute grant.

397

### 398 **References**

399 Aničić, M., Spasić, T., Tomašević, M., Rajšić, S., Tasić, M., 2011. Trace elements  
400 accumulation and temporal trends in leaves of urban deciduous trees (*Aesculus*  
401 *hippocastanum* and *Tilia* spp.). Ecological Indicators 11, 824-830.

402

403 Antosiewicz, D.M., Escudé-Duran, C., Wierzbowska, E., Skłodowska, A., 2008. Indigenous  
 404 plant species with the potential for the phytoremediation of arsenic and metals contaminated  
 405 soil. *Water Air and Soil Pollution* 193, 197–210.  
 406  
 407 Baker, A.J.M., McGrath, S.P., Reeves, R.D., Smith, J.A.C., 2000. Metal hyperaccumulator  
 408 plants: a review of the ecology and physiology of a biological resource for phytoremediation  
 409 of metal polluted-soils. In: Terry, N., Bañuelos, G., Eds., *Phytoremediation*  
 410 *of Contaminated Soil and Water*. Lewis Publishers, London, pp. 85-107.  
 411  
 412 Bargagli, R., 1998. *Trace Elements in Terrestrial Plants: An Ecophysiological Approach to*  
 413 *Biomonitoring and Biorecovery*. Springer-Verlag, Berlin.  
 414  
 415 Bargagli, R., Monaci, F., Agnorelli, C., 2003. Oak leaves as accumulators of airborne  
 416 elements in an area with geochemical and geothermal anomalies. *Environmental Pollution*  
 417 124, 321-329.  
 418  
 419 Barker, A.V., Pilbeam, D.J. (Eds.), 2010. *Handbook of Plant Nutrition*. Taylor and Francis,  
 420 Boca Raton, FL.  
 421  
 422 Bull, A., Brown, M.T., Turner, A., 2017. Novel use of field-portable-XRF for the direct  
 423 analysis of trace elements in marine macroalgae. *Environmental Pollution* 220, 228-233.  
 424  
 425 Dimitrijević, M.D., Nujkić, M.M., Alagić, S.C., Milić, S.M., Tošić, S.B., 2016. Heavy metal  
 426 contamination of topsoil and parts of peach-tree growing at different distances from a  
 427 smelting complex. *International Journal of Environmental Science and Technology* 13, 615-  
 428 630.

429

430 Dmuchowski, W., Gozdowski, D., Bragoszewska, P., Baczewska, A.H., Suwara, I., 2014.

431 Phytoremediation of zinc contaminated soils using silver birch (*Betula pendula* Roth).

432 Ecological Engineering 71, 32-35.

433

434 Environmental Protection Agency, 2007. Method 6200 - Field portable x-ray fluorescence

435 spectrometry for the determination of elemental concentrations in soil and sediment.

436 <http://www3.epa.gov/epawaste/hazard/testmethods/sw846/pdfs/6200.pdf>. Accessed 7/16.

437

438 Franiel, I., Babczyńska, A., 2011. The growth and reproductive effort of *Betula*

439 *pendula* Roth in a heavy-metals polluted area. Polish Journal of Environmental Studies 20,

440 1097-1101.

441

442 Hubbell, J.H., Seltzer, S.M., 1996. X-ray mass attenuation coefficients. National Institute of

443 Standards and Technology, Gaithersburg, Maryland.

444

445 Kabata-Pendias, A., Pendias, H., 2001. Trace Elements in Soils and Plants, third ed. CRC

446 Press, Boca Raton, Florida, USA.

447

448 Kalnicky, D.J., Singhvi, R., 2001. Field portable XRF analysis of environmental samples.

449 Journal of Hazardous Materials 83, 93-122.

450

451 Madejón, P., Marañón, Murillo, J.M., Robinson, B., 2004. White poplar (*Populus alba*) as a

452 biomonitor of trace elements in contaminated riparian forests. Environmental Pollution 132,

453 145-155.

454

Nirola, R., Megharaj, M., Palanisami, T., Arjal, R., Venkateswarlu, K., Naidu, R., 2015. Evaluation of metal uptake factors of native trees colonizing an abandoned copper mine e a quest for phytostabilization. *Journal of Sustainable Mining* 14, 115-123.

Pająk, M., Halecki, W., Gąsioer, M., 2017. Accumulative response of Scots pine (*Pinus sylvestris* L.) and silver birch (*Betula pendula* Roth) to heavy metals enhanced by Pb-Zn ore mining and processing plants: Explicitly spatial considerations of ordinary kriging based on a GIS approach. *Chemosphere* 168, 851-859.

Radu, T., Diamond, D., 2009. Comparison of soil pollution concentrations determined using AAS and portable XRF techniques. *Journal of Hazardous Materials* 171, 1168–1171.

Rawlins, B.G., O'Donnell, K., Ingham, M., 2003. Geochemical survey of the Tamar catchment (south-west England). *British Geological Survey Report CR/03/027*, 232pp.

Sacristán, D., Viscarra Rossel, R.A., Recatalá, L., 2016. Proximal sensing of Cu in soil and lettuce using portable X-ray fluorescence spectrometry. *Geoderma* 265, 6-11.

Schmidt, M., Boras, S., Tjoa, A., Watanabe, T., Jansen, S., 2016. Aluminium accumulation and intra-tree distribution patterns in three *Arbor aluminosa* (*Symplocos*) Species from Central Sulawesi. *PLOS ONE* <https://doi.org/10.1371/journal.pone.0149078>

Serbula, S.M., Radojevic, A.A., Kalinovic, J.V., Kalinovic, T.S., 2014. Indication of airborne pollution by birch and spruce in the vicinity of copper smelter. *Environmental Science nad Pollution Research* 21, 11510-11520.

481 Stefanowicz, A.M., Stanek, M., Woch, M.W., 2016. High concentrations of heavy metals in  
482 beech forest understory plants growing on waste heaps left by Zn-Pb ore mining. *Journal of*  
483 *Geochemical Exploration* 169, 157-162.  
484  
485 Towett, E.K., Shepherd, K.D. and Drake, B.L., 2016. Plant elemental composition and  
486 portable X-ray fluorescence (pXRF) spectroscopy: quantification under different  
487 analytical parameters. *X-ray Spectrometry* 45, 117-124.  
488  
489 Turner, A., Poon, H., Taylor, A., Brown, M.T., 2017. In situ determination of trace elements  
490 in *Fucus* spp. by field-portable-XRF. *Science of the Total Environment* 593-594, 227-235.  
491  
492 Unterbrunner, R., Puschenreiter, M., Sommer, P., Wieshammer, G., Tlustos, P., Zupan, M.,  
493 Wenzel, W.W., 2007. Heavy metal accumulation in trees growing on contaminated sites in  
494 central Europe. *Environmental Pollution* 148, 107-114.  
495

Table 1: A comparison of measured and certified elemental concentrations in plastic, leaves and soils. Errors represent the 95% confidence interval, with weighting for inter-method variance where appropriate (certified), or two standard deviations about the mean (measured  $n$  times); asterisks denote indicative values.

		certified, $\mu\text{g g}^{-1}$ dw	measured, $\mu\text{g g}^{-1}$ dw
polyethylene disc, PN 180-619 XRF; $n = 10$	As	$51 \pm 7.0$	$46 \pm 4.4$
	Pb	$150 \pm 12$	$145 \pm 9.2$
peach leaves, GBW 08501 ICP; $n = 3$	As	$0.34 \pm 0.06$	$0.44 \pm 0.04$
	Cu	$10.4 \pm 1.6$	$8.0 \pm 0.42$
	Pb	$0.99 \pm 0.08$	$0.96 \pm 0.04$
	Zn	$22.8 \pm 2.5$	$23.3 \pm 7.4$
soil, NIST 2709 XRF; $n = 5$	As	$10.5 \pm 0.3^*$	$9.3 \pm 2.3$
	Cu	$33.9 \pm 0.5^*$	$26.3 \pm 6.1$
	Pb	$17.3 \pm 0.1$	$12.9 \pm 3.4$
	Zn	$103 \pm 4.0^*$	$97.5 \pm 8.1$
soil, MSH-100 XRF; $n = 5$	As	$1090 \pm 16.7$	$999 \pm 24.0$
	Zn	$1100 \pm 16.8$	$1047 \pm 36.0$

Table 2: Number and distribution of leaf samples used in the present study.

sampling site	<i>Fagus</i>	<i>Betula</i> spp.	<i>Quercus</i> spp.
S1	15	9	9
S2	3	3	12
S3	9	18	9
total	27	30	30

Table 3: A summary of the characteristics of the soil samples from the three sites, shown as the mean and one standard deviation for each parameter.

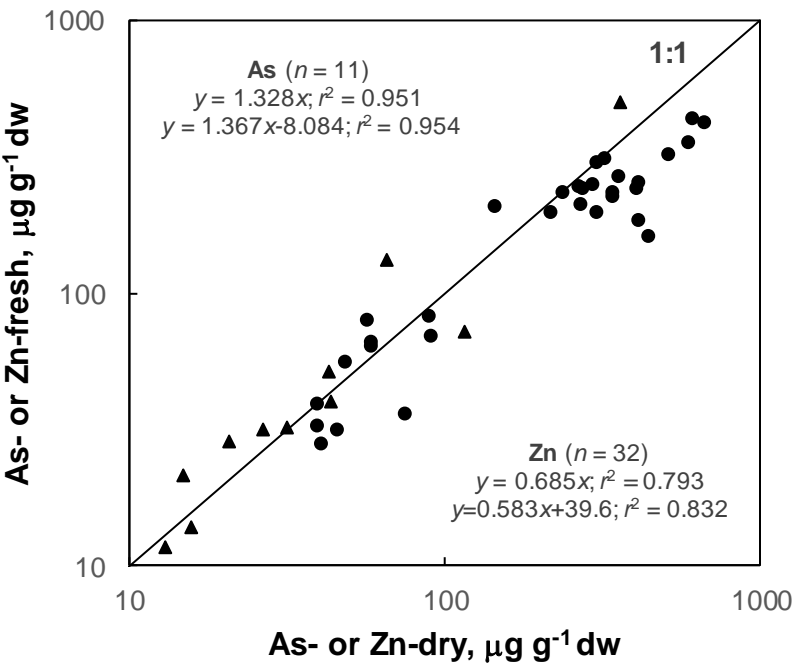
sampling site	pH	As, $\mu\text{g g}^{-1}$ dw	Cu, $\mu\text{g g}^{-1}$ dw	Pb, $\mu\text{g g}^{-1}$ dw	Zn, $\mu\text{g g}^{-1}$ dw
S1 ( $n = 3$ )	$5.53 \pm 0.68$	$183 \pm 60$	$356 \pm 192$	$103 \pm 34.1$	$192 \pm 35.3$
S2 ( $n = 3$ )	$4.89 \pm 0.83$	$9310 \pm 8470$	$1070 \pm 858$	$159 \pm 73$	$125 \pm 33.9$
S3 ( $n = 3$ )	$5.40 \pm 0.74$	$24,200 \pm 6620$	$1380 \pm 453$	$254 \pm 44.9$	$187 \pm 89$

Table 4: Mean and, in parentheses, minimum and maximum XRF measurement detection limits for trace elements in fresh and freeze-dried leaf samples.

	As	Cu	Pb	Zn
fresh ( $n = 87$ ), $\mu\text{g g}^{-1}$ fw	12.9 (4.5-47.9)	71.3 (29.2-215)	26.7 (10.9-83.4)	33.5 (15.6-113)
dry ( $n = 87$ ), $\mu\text{g g}^{-1}$ dw	21.2 (9.9-52.9)	116 (59.1-353)	42.9 (19.2-118)	56.9 (22.6-189)

Table 5: The number of cases that each element was detected among the leaf samples analysed ( $n$ ) and summary statistics for the resulting concentrations.

		As	Cu	Pb	Zn
XRF-fresh, $\mu\text{g g}^{-1}$ fw	$n$	19	0	0	40
	mean	47.5			92.4
	median	20.3			89.3
	min	5.2			21.0
	max	450			280
XRF-fresh, $\mu\text{g g}^{-1}$ dw	$n$	19	0	0	40
	mean	60.0			169
	median	28.4			192
	min	11.7			28.0
	max	501			436
XRF-dry, $\mu\text{g g}^{-1}$ dw	$n$	13	2	0	47
	mean	63.5	71.3		208
	median	37.6	71.3		175
	min	12.9	62.0		27.6
	max	361	80.6		661
ICP, $\mu\text{g g}^{-1}$ dw	$n$	28	28	28	28
	mean	28.0	12.9	4.4	76.6
	median	1.4	8.7	2.4	23.1
	min	0.04	3.7	0.52	2.7
	max	503	85.6	25.6	344



520

521

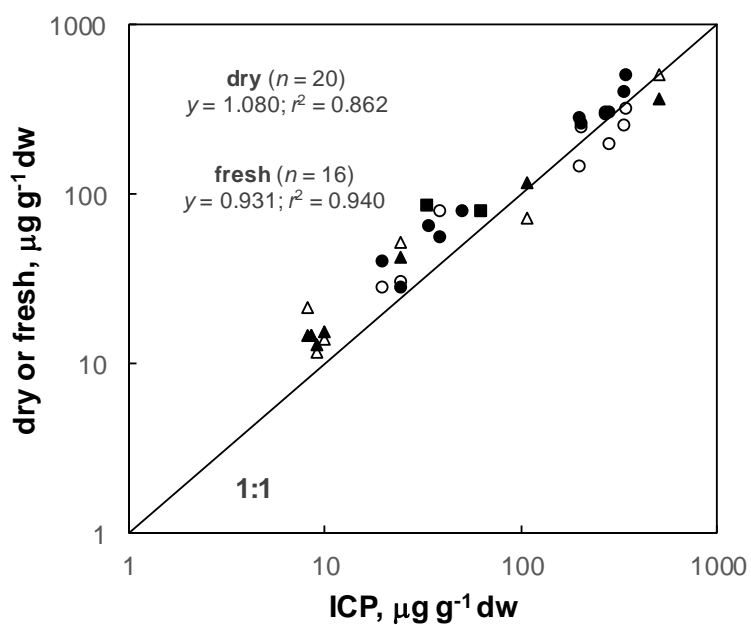
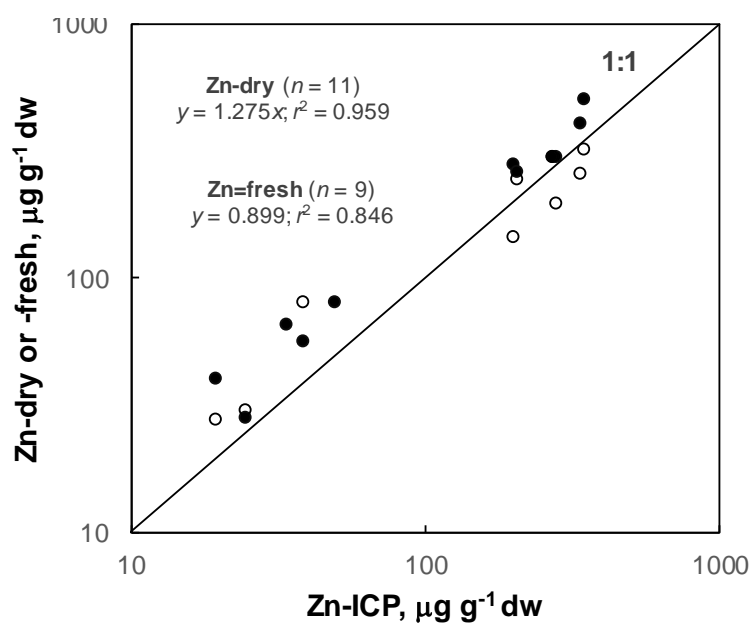
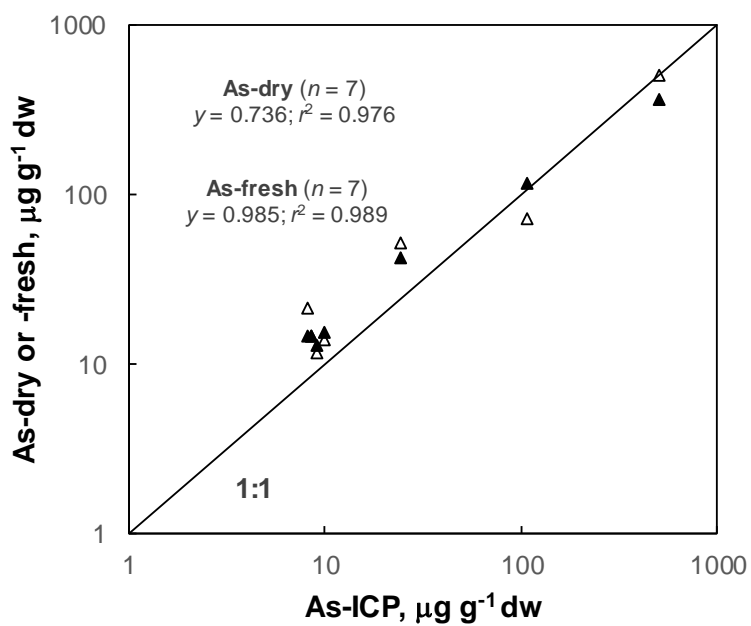
522 Figure 1: A comparison of dry weight leaf concentrations of As ( $\blacktriangle$ ) and Zn ( $\bullet$ ) derived from  
523 fresh analysis by XRF and correction for water content and returned by direct analysis by  
524 XRF. The solid line denotes unit slope and regression equations and coefficients of  
525 determination defining the data sets are annotated.

526

527



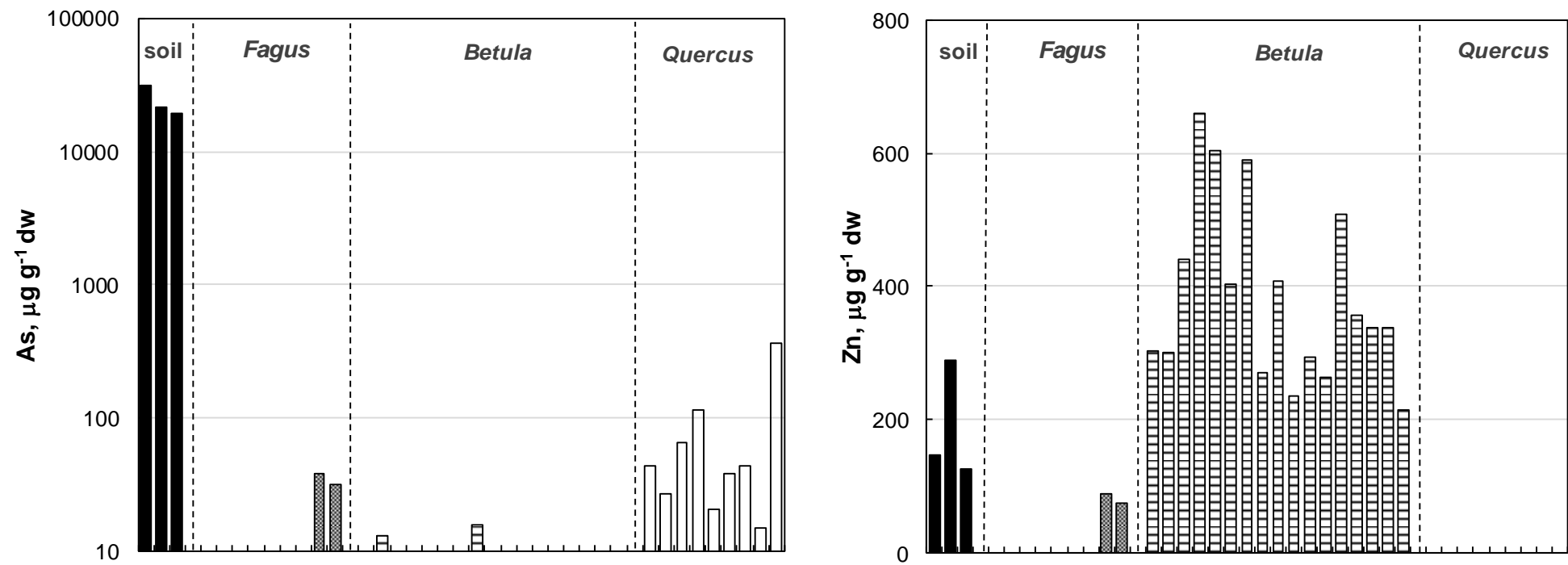




530

531 Figure 2: A comparison of the dry weight concentrations of trace elements in leaves  
532 determined by ICP following acid digestion and by XRF (As analysed fresh,  $\Delta$ , and dry,  $\blacktriangle$ ;  
533 Zn analysed fresh,  $\circ$ , and dry,  $\bullet$ ; Cu analysed dry,  $\blacksquare$ ). The solid line denotes unit slope and  
534 regression equations and coefficients of determination defining the data sets are annotated.

535 Figure 3: Concentrations of As and Zn, where detected, in the individual soil and tree leaf samples from S3.



536  
537  
538